

Study of MHD destabilization and injection penetration of Shattered Pellet Injection by JOEKE 3D reduced MHD simulation

PPPL workshop 2017-07

Di Hu (胡地, Di.Hu@iter.org)

Collaborators: E. Nardon, M. Lehnen,
G.T.A. Huijsmans, D. C. van Vugt.

Acknowledgement: A. Boozer, S. Cristian, R. Sweeney.

Science Division. ITER Organisation
Route de Vinon-sur-Verdon, CS 90 046
13067 St. Paul-lez-Durance, France.

*The views and opinions expressed herein
DO NOT necessarily reflect those of the ITER organization.*

PPPL workshop, 2017 July, Princeton, NJ, USA

Abstract

- The deuterium deposition, cooling and ensuing large scale MHD instability caused by Shattered Pellets Injection (SPI) are investigated in this study.
- The primary MHD destabilization mechanism of deuterium SPI is identified as the local helical cooling of rational surfaces.
- The SPI penetration is found to be much better than the same quantity MGI into the same equilibrium. MHD mixing are found to be beneficial for the penetration.
- The impact of injection parameter of SPI is investigated for different shard size, injection velocity, spread angle and injection amount.
- The penetration depth for different equilibrium temperature before the thermal quench is investigated using the same SPI parameters.
- The large mode number modes and their interaction with the macroscopic modes are beyond the scope of this study.

Contents

- 1 Introduction
- 2 System of interest
 - Governing equations
 - Reference parameters
- 3 MHD activities
 - Destabilizing mechanism of SPI
 - Difference in MHD behavior between MGI and SPI case
 - Destruction and recovery of flux surfaces during SPI
- 4 Penetration & Assimilation of SPI
 - Comparison between MGI & SPI penetration
 - Impact of injection parameters
 - Comparison between different temperature
- 5 Conclusion

SPI as disruption mitigation schemes

- Shattered Pellet Injection (SPI) is the baseline concept for ITER disruption mitigation, aiming to inject about 10^{25} neutral atoms within milliseconds (basically a shotgun).
- The deposition of pellet contents cools the plasma by dilution and radiation, induces corresponding current perturbation, destabilizes macroscopic current driven instabilities and break flux surfaces.
- It is desirable to deposit most of contents right into the core of plasma before triggering thermal quench, so that the thermal energy can be radiated away uniformly.
- Local pressure gradient caused by injection may also cause local pressure driven instabilities, but unlikely to cause global confinement destruction by themselves.
- We hereby consider the deuterium SPI into a JET L mode plasma to study both the MHD and the injection deposition.

Reduced MHD equations with neutrals

The 3D reduced MHD with diffusive neutrals is used to describe the dynamics. Neutral convective effects are absent.

$$\mathbf{B} = F_0 \nabla \phi + \nabla \psi \times \nabla \phi, \quad (1)$$

$$\mathbf{v} = \mathbf{v}_\perp + v_\parallel \mathbf{B} = R^2 \nabla \phi \times \nabla u + v_\parallel \mathbf{B}. \quad (2)$$

And the governing equations in (R, Z, φ) coordinates are:

$$\frac{\partial \psi}{\partial t} = \eta(T) \Delta^* \psi - R\{u, \psi\} - F_0 \frac{\partial u}{\partial \phi}, \quad (3)$$

$$j = \Delta^* \psi, \quad j_\phi = -j/R, \quad (4)$$

$$\begin{aligned} R \nabla \cdot \left(R^2 \rho \nabla_{pol} \frac{\partial u}{\partial t} \right) &= \frac{1}{2} \left\{ R^2 |\nabla_{pol} u|^2, R^2 \rho \right\} + \{R^4 \rho \omega, u\} + \{\psi, j\} \\ &\quad - \frac{F_0}{R} \frac{\partial j}{\partial \phi} + \{\rho T, R^2\} + R \mu(T) \nabla^2 \omega \\ &\quad - \nabla \cdot \left[(\rho \rho_n S_{ion}(T) - \rho^2 \alpha_{rec}(T)) R^2 \nabla_{pol} u \right] \quad (5) \end{aligned}$$

Reduced MHD equations with neutrals (cont.)

Continuing from previous slice,

$$\omega = \frac{1}{R} \frac{\partial}{\partial R} \left(R \frac{\partial u}{\partial R} \right) + \frac{\partial^2 u}{\partial Z^2}, \quad (6)$$

$$\begin{aligned} \frac{\partial \rho}{\partial t} = & -\nabla \cdot (\rho \mathbf{v}) + \nabla \cdot (D_{\perp} \nabla_{\perp} \rho + D_{\parallel} \nabla_{\parallel} \rho) \\ & + \rho \rho_n S_{ion}(T) - \rho^2 \alpha_{rec}(T), \end{aligned} \quad (7)$$

$$\begin{aligned} \frac{\partial (\rho T)}{\partial t} = & -\mathbf{v} \cdot \nabla (\rho T) - \gamma \rho T \nabla \cdot \mathbf{v} + \frac{2}{3R^2} \eta(T) J^2 \\ & + \nabla \cdot (\kappa_{\perp} \nabla_{\perp} T + k_{\parallel} \nabla_{\parallel} T) - \xi_{ion} \rho \rho_n S_{ion}(T) \\ & - \rho \rho_n P_L(T) - \rho^2 P_B(T), \end{aligned} \quad (8)$$

$$\begin{aligned} \rho B^2 \frac{\partial v_{\parallel}}{\partial t} = & -\rho \frac{F_0}{2R^2} \frac{\partial}{\partial \phi} (B^2 v_{\parallel}^2) - \frac{\rho}{2R} \{B^2 v_{\parallel}^2, \psi\} - \frac{F_0}{R^2} \frac{\partial (\rho T)}{\partial \phi} \\ & + \frac{1}{R} \{ \psi, \rho T \} + B^2 \mu_{\parallel}(T) \nabla_{pol}^2 v_{\parallel} \\ & + (\rho^2 \alpha_{rec}(T) - \rho \rho_n S_{ion}(T)) B^2 v_{\parallel}, \end{aligned} \quad (9)$$

$$\frac{\partial \rho n}{\partial t} = \nabla \cdot (\mathbf{D} : \nabla \rho n) - \rho \rho_n S_{ion}(T) + \rho^2 \alpha_{rec}(T) + S_n. \quad (10)$$

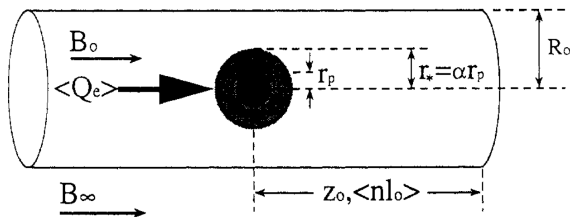
Here, S_{ion} and α_{rec} are the ionization and recombination rate, respectively, while $\xi_{ion} = 13.6\text{eV}$ is the ionization energy of deuterium. Further, P_L and P_B are the line radiation and bremsstrahlung radiation rate coefficient respectively.

Implementation of NGS model for deuterium

- The ablation rate of a single shard is acquired by using NGS model for given pellet radius, electron density and electron temperature.

$$\partial_t N [s^{-1}] = 4.12 \times 10^{16} r_p^{4/3} [m] n_e^{1/3} [m^{-3}] T_e^{1.64} [eV]. \quad (11)$$

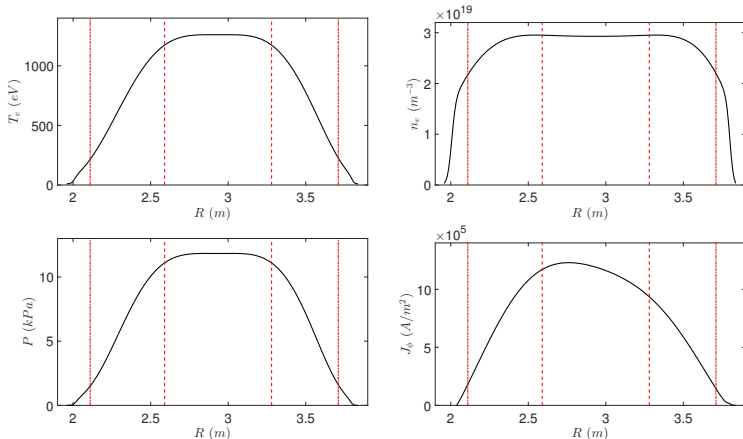
- The shard radius evolution is governed by the conservation of mass.
- The ablation is self-regulated so long the plasma remains Maxwellian.



B. Pégourié et al, Nucl. Fusion, 1993; B. Pégourié et al, Plasma Phys. Control. Fusion, 2005.

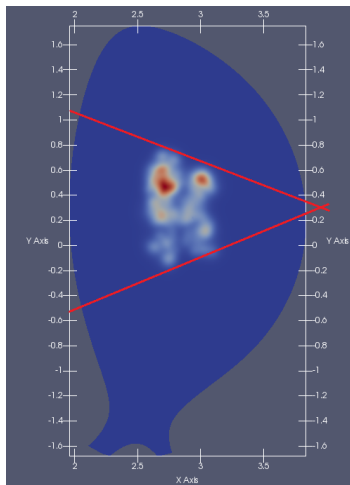
The standard target equilibrium

We use the JET shot 86887 as a template for the target equilibrium with $q_0 = 0.935$ and $q_{95} = 2.9$. The toroidal magnetic field $B_t = 2T$, and the total plasma current is $I_p = 2MA$. Not a high performance plasma.



Reference injection parameters

- The total injected deuterium is on the order of 0.5×10^{23} atoms.
- The pellet is equally shattered into 100 shards, each with radius 1.26mm with speed $500 \pm 100\text{m/s}$.
- The spread vertex angle of SPI is set to be 40 degrees.
- The reference injection direction is purely along major radial for now.
- The injection is carried out on the LFS.
- This injection configuration does not exactly reflect the real JET system.
- Various alternative injection parameter will be compared later in this study.



Current redistribution caused by cooling

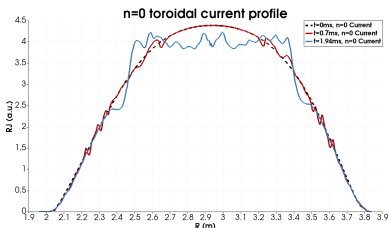
- Macroscopic current driven modes are the main players in the global confinement destruction.
- Plasma cooling perturbs the current profile by the diffusion-like behavior of the electric field profile.

$$R \frac{\partial}{\partial t} E_\phi = \eta \Delta^* (R E_\phi) + \dots, \quad E_\phi = \eta (T_e) j_\phi + \dots. \quad (12)$$

- Since $\eta \propto T_e^{-3/2}$, the current density will be pushed from low temperature region into the high temperature region.
- The current redistribution timescale is $\tau_j \sim L^2 \eta^{-1}$, where L is the characteristic length scale of said redistribution.
- Hence the classic picture of injection destabilization is directly linked to the global current contraction.
- For deuterium SPI however, the local perturbation at rational surfaces rather than global current contraction is more dominant.

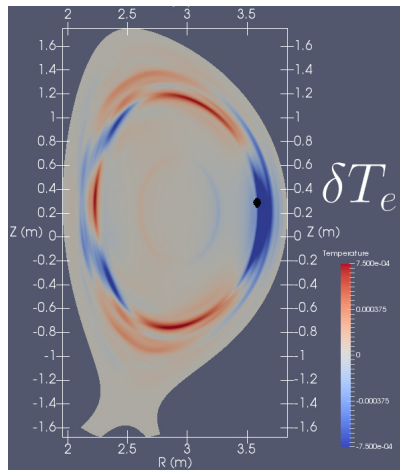
The evolution of $n = 0$ plasma current density

- Before TQ, the global current contraction is limited due to small deuterium radiation, thus long global current contraction time.
- However, jagged local current redistribution occurs near resonant surfaces as a result of helical cooling. The local helical cooling is found to be the major destabilising mechanism.
- Mean current flattened in the core of plasma by hyper-resistivity.



The development of helical structure

- The electron temperature is flattened along the field lines by parallel conduction.
- On irrational surface, the whole surface is cooled down.
- Near rational surface, helical concentration of cooling occurs instead due to periodicity, which relaxes in a perpendicular transport timescale.
- Such helical cooling results in helical current redistribution which is detrimental to MHD stabilities for resonant modes at corresponding surfaces.



Impact to the stability

- The stability of macroscopic tearing or resistive kink modes are sensitive to local mode structure near resonant surface.
- The impact of this resonant current perturbation can be seen by looking at the mode structure of a single helicity mode,

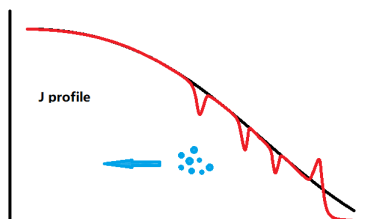
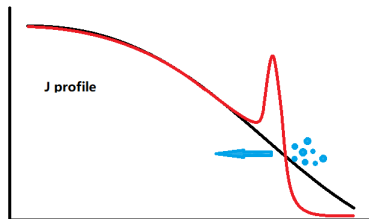
$$\Psi^* = \Psi_0^* + \psi, \quad \frac{1}{r} \frac{\partial}{\partial r} \left(r \frac{\partial}{\partial r} \psi \right) = - \langle j^* \rangle_1 + \frac{m^2}{r^2} \psi, \quad (13)$$

where the j^* is the helical current. In the linear no pressure limit we have $\langle j^* \rangle_1 = d \langle j^* \rangle_0 / d \langle \Psi^* \rangle_0 \psi$ which yield the linear eigen-equation for the outer solution of the mode. The choice of sign is such that j^* and Ψ''_{0s} are negative and ψ is positive.

- The stability is determined by $\Delta' \equiv \left. \frac{\psi'_s}{\psi_s} \right|_{-}^{+}$. It can be seen that the m^2 term is always stabilizing as it raises $\psi'_s|_{-}$ while decreases $\psi'_s|_{+}$.
- On the other hand, a helical current decrease, thus positive $\langle j^* \rangle_1$, will always be destabilizing as it lowers $\psi'_s|_{-}$ and increases $\psi'_s|_{+}$.

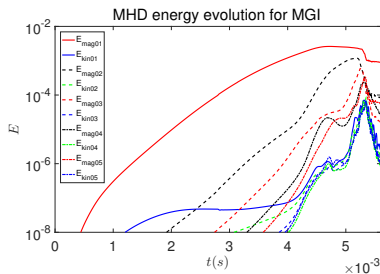
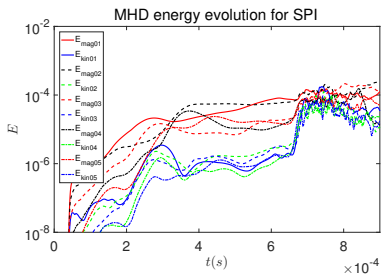
Local cooling vs. global contraction

- The competition between those two mechanisms is governed by the comparison of the global current contraction timescale and the pellets travel timescale.
- If the global current contraction time is quick comparing with pellets travel time, the contraction follows closely with the shards, and little current density is left to be disturbed locally.
- Otherwise, the local current displacement **always** occurs faster due to the much smaller length scale.



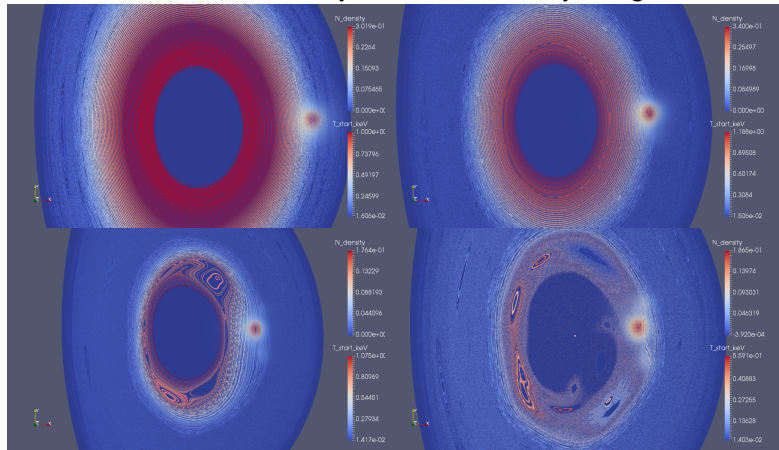
Different behaviors in mode energy evolution

- Same quantity injection into the standard equilibrium.
- For MGI case, the 2/1 mode is dominant. When this dominant mode is large enough ($E_{mag} > 10^{-3}$), it will drive up the other modes and trigger the thermal quench.
- For SPI case, the perturbation spectrum is much broader as there is no dominant mode. The development of multiple modes triggers the thermal quench at a relative low amplitude ($E_{mag} \sim 10^{-4}$).
- The SPI spectrum resembles that of the MGI if the pellets are slow.



Poincare plots as the pellets travel across the plasma

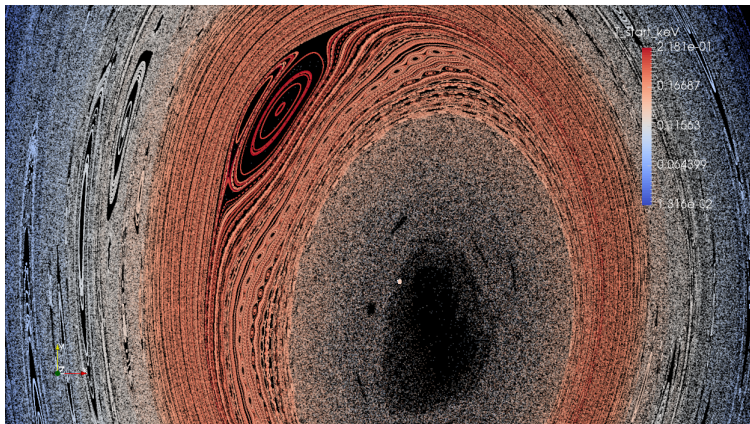
As a result of helical cooling, the pellets destabilize a wide spectrum of modes in their wake and destroy the flux surfaces by doing so.



The poincare plot for 0.3ms, 0.6ms, 0.8ms (TQ) & 0.9ms, respectively.

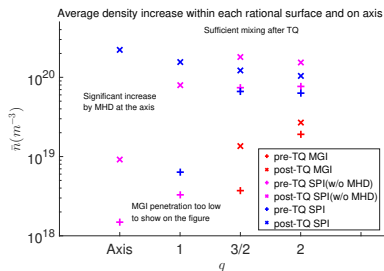
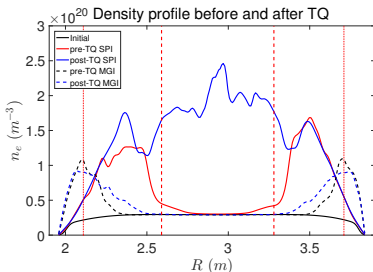
Partial recovery of flux surfaces after thermal quench

Partial flux surfaces healing observed numerically milliseconds after the onset of thermal quench ($t = 1.8ms.$).



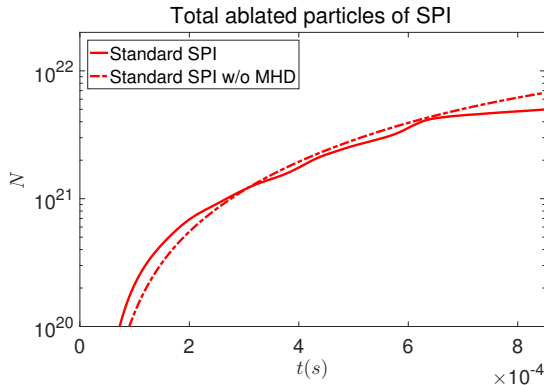
The penetration of injection

- Here we compare the penetration at the axis and into $q = 1, 3/2$ and 2 surface for MGI and SPI just before and after the onset of TQ.
- The SPI without MHD instabilities are compared to see the impact of MHD, which is found to be beneficial to the core penetration.
- The SPI core penetration is found to be much better than the MGI.
- The TQ period is from $0.67ms$ to $1.05ms$ for the SPI and $5.37ms$ to $6.07ms$ for the MGI.



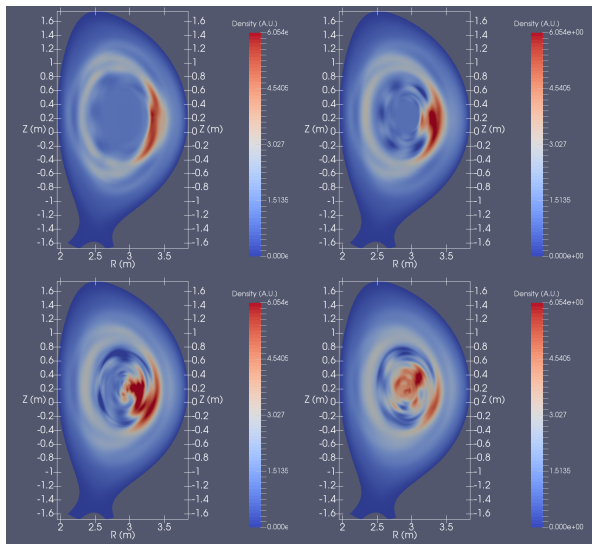
The assimilation of SPI with and without MHD

- The total number of ablated particles differs only slightly between the with and without MHD cases.
- Any differences shown in the penetration between those two cases are purely caused by the additional transport of MHD activities.



Convective mixing within $q = 1$ surface

For the SPI case, a strong **convective** density flux is identified as the 1/1 kink goes unstable. The 1/1 kink mode provides efficient mixing in the core region, contributes to the significant density increase near the magnetic axis.



The density contour for 0.72ms, 0.80ms, 0.88ms & 1.00ms, respectively.

The impact of the shattering process

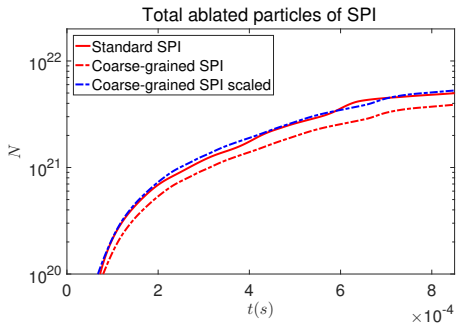
- Naively looking at the ablation scaling law, one would expect the total ablation rate goes up with $r_{shard}^{-5/3}$ since we have:

$$N'_{shard} \propto r_{shard}^{4/3}, \quad n_{shard} \propto r_{shard}^{-3}. \quad (14)$$

- The total ablation rate $N'_{total} = n_{shard} N'_{shard} \propto r_{shard}^{-5/3}$.
- However, as the ablated materials cool the plasma down, this strong dependent scaling is not suppose to hold exactly.
- Preliminary result shows a $r_{shard}^{-2/3}$ scaling instead, but this is by no means a serious scaling law study, but rather to show that we should not expect the same result with what we will get from simply looking at the ablation rate scaling.

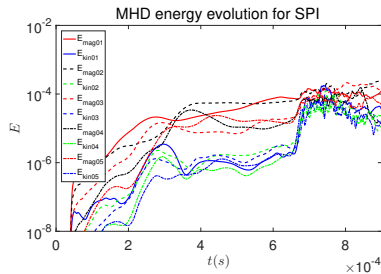
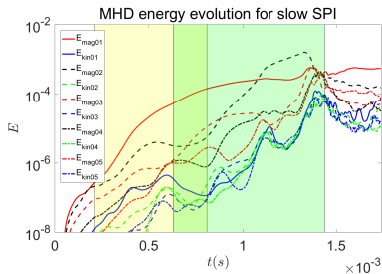
The impact of the shattering process (cont.)

- The standard SPI ablation rate is compared with a “coarse-grained” SPI case with the same total injection amount but fewer shards ($n_{shards} = 20$) each with larger radius ($r_{shards} = 2mm$).
- The coarse-grained SPI ablation scaled with $r_{shard}^{-2/3}$ is also shown. Further investigation is needed for serious scaling law.



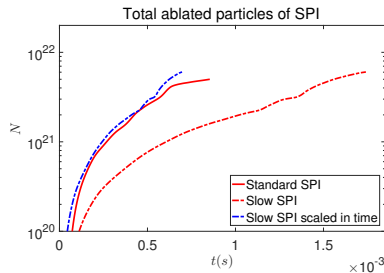
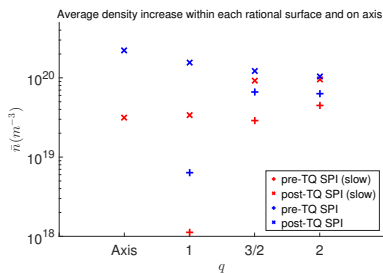
The impact of the injection velocity (MHD)

- Varying the injection speed will have a impact on the MHD since the time shards spend near a given rational surface will change.
- A slow SPI with reference speed $200 \pm 40 \text{ m/s}$ but otherwise the same parameter is compared with the standard SPI.
- Green and yellow patches denote the time period the shards spend near $q = 3/2$ and $q = 2$ surface respectively.
- For the slow SPI, the thermal quench is triggered as the growing stochastic region reaches the $q = 1$ surface.



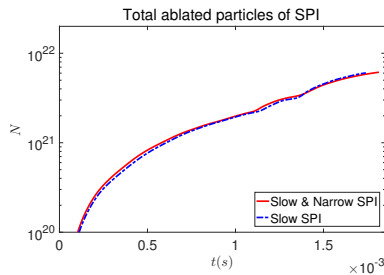
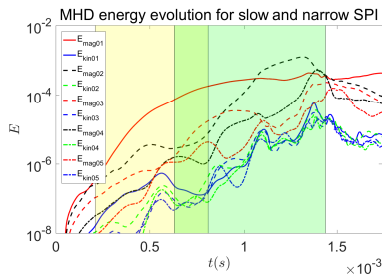
The impact of the injection velocity (Assimilation)

- The thermal quench is triggered before the shards reach the $q = 1$ surface, and the peak of magnetic perturbation is near $q = 3/2$ and $q = 2$ surface, rather than deep in the core.
- As a result, the inward particle flux caused by MHD mixing is much weaker comparing to the standard SPI case.
- The total ablated particles for the standard SPI and slow SPI are compared. The slow SPI case is also scaled by the velocity to provide a sense of assimilation for a given distance travelled by the shards.



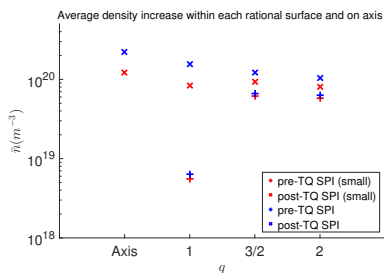
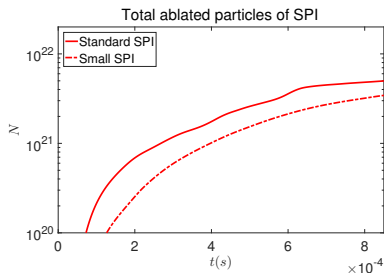
The impact of the spread angle (MHD & assimilation)

- The spread angle might affect the MHD since a wider spread angle eliminates higher order harmonics in the perturbed helical current.
- A slow & narrow SPI with spread angle 20° but otherwise the same parameters with the slow SPI is introduced to investigate this effect.
- Only slight changes in the MHD spectrum, almost identical assimilation rate. Varying the spread angle within reasonable range does not make any significant impact.



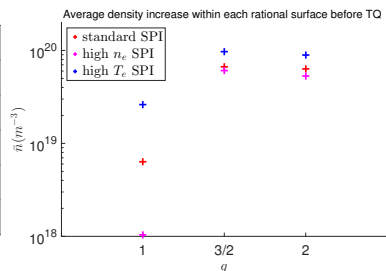
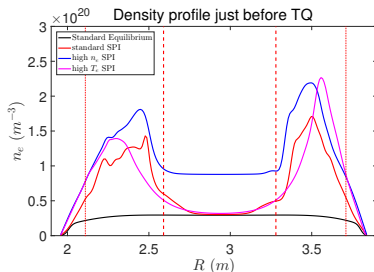
Assimilation, penetration and total injection quantity

- A small amount SPI with 6.25×10^{21} atoms but otherwise the same parameters is compared with the standard SPI to investigate the assimilation rate as a function of total injection amount.
- The total amount of ablated particles only increase weakly with the total injection amount, thus decreasing assimilation fraction.
- Similar MHD mixing and penetration behavior comparing with the standard amount of injection.



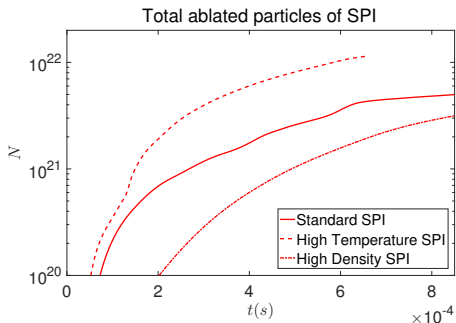
The penetration of injection for different T_{e0}

- We compare the injection penetration just before the TQ for three equilibria with the same shape of T_e and n_e profile, the standard equilibrium, the high n_e equilibrium with $T_e(0) = 420\text{eV}$, $n_e(0) = 8.7 \times 10^{19} \text{m}^{-3}$, and a high T_e equilibrium with $T_e(0) = 3.75\text{keV}$, $n_e(0) = 2.9 \times 10^{19} \text{m}^{-3}$. We assume $T_e = T_i$.
- The assimilation & penetration before the TQ depend weakly on T_e . This is possibly due to an earlier TQ and the thermal shielding of the periphery shards in the pellet cloud (need more study).



The assimilation for different T_{e0}

- The total assimilation does not follow the $T_e^{1.64}$ power law of the NGS model, but have a weaker scaling instead.
- For the high n_e case, the assimilation at the time of TQ shows a weak dependence on T_e , despite the same total thermal energy.
- For the high T_e case, the assimilation approximately doubles for triple the temperature and thermal energy.



Conclusion

- Local helical cooling is found to be the main destabilizing mechanism for deuterium SPI, as opposed to the global current contraction.
- The resulting MHD modes are milder but has a broad spectrum.
- Much better injection penetration is found for SPI comparing with MGI. For SPI, sufficient mixing occurs during TQ, raising the central density to be higher than the average density. While MGI is concentrated on the outer region even after TQ.
- MHD activities are found to be beneficial to the penetration.
- The impact of various injection parameters to the MHD activities, penetration and assimilation is investigated. Most notably, the fineness of shattering can impact the total assimilation fraction, and the injection velocity has a impact on MHD activities and consequentially the core penetration.
- The particle number increase just before TQ has a relatively weak dependence on the equilibrium temperature and thermal energy, possibly due to the thermal shielding of periphery shards.

Backup Slides

Turbulent wake drag caused by the background plasma

- The drag force experienced by an object in unmagnetized fluid is

$$F_d = \frac{1}{2} \rho_f v_p^2 C_d A. \quad (15)$$

- In our case, additional contribution from perturbed magnetic field have to be considered, but should be on the same order of magnitude as the kinetic contribution due to the equipartition of energies.
- The spherical pellet mass is

$$M_p = \frac{4}{3} \pi r_p^3 \rho_p. \quad (16)$$

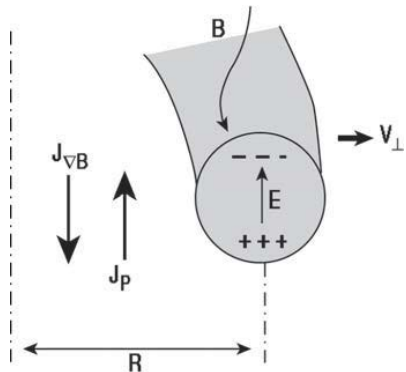
- Thus the time scale of drag force is

$$\tau_d = v \frac{M_p}{F_d} = \frac{8}{3} \frac{\rho_p}{\rho_f} \frac{r_p}{v_p} C_d^{-1}. \quad (17)$$

- The huge difference in density between pellets and plasmas means the pellets can be seen as effectively dragless.

Polarization of ablated materials and major radius drift

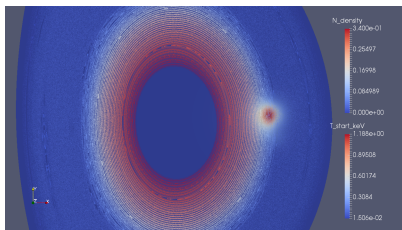
- The ablation of pellet materials create a shielding cloud of neutral gas, which further create a tube of cool but high pressure plasmas upon ionization.
- This localized high pressure region cause diamagnetic effect, thus result in a imbalance of ∇B and curvature drift with the background plasma.
- The net vertical current leads to the polarization of the cool plasma tube, further result in a $\vec{E} \times \vec{B}$ drift pointing to the major radial direction.
- The drift act on ablated plasmas rather than pellet itself.



P. B. Park et al., Phys. Plasmas, 2000.

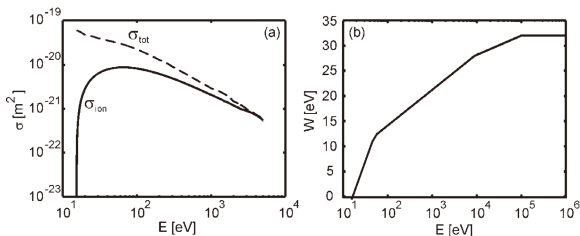
Factors that undermine the major radial drift

- The local high pressure region relaxes with the time scale corresponding to sound velocity travelling along field lines.
- The nested flux surface indicate that after long enough distance along the field lines, the positive electric potential region will connect with the negative region, neutralizing the $\vec{E} \times \vec{B}$ drift.
- It is observed numerically that shattered pellets stir up a broader spectrum of modes that its MGI counterpart, and the flux surfaces in the wake of shattered pellets become stochastic quickly.



Slow down of 10keV electrons

In a Maxwellian plasma, the ablation rate can always self-adjust to create a dense enough shielding so long as the particle mean free path is small comparing with the pellet size.



For 10keV electrons, σ is above 10^{-22}m^2 , $n_p \sim \mathcal{O}(10^{28}/\text{m}^3)$, hence the mean free path is $\lambda = (\sigma n_p)^{-1} \sim \mathcal{O}(10^{-6} \text{m})$. The collision frequency, thus the slowing down time, is weakly dependent on T_e for a given mean free path since $\nu_e = v_{th}/\lambda \propto T_e^{-1/2}$.

B. Pégourié et al, Plasma Phys. Control. Fusion, 2005.